

# High resolution interferometer with multiple-pass optical configuration

Jeongho Ahn,<sup>1</sup> Jong-Ahn Kim,<sup>2</sup> Chu-Shik Kang,<sup>2</sup> Jae-Wan Kim,<sup>2\*</sup> and Soohyun Kim<sup>1\*</sup>

<sup>1</sup>*Division of Mechanical Engineering, KAIST, 335 Gwahangno, Yuseong-gu, Daejeon, 305-701, Republic of Korea*

<sup>2</sup>*Center for Length & Time, KRISS, 209 Gwahangno, Yuseong-gu, Daejeon, 305-340, Republic of Korea*

<sup>2</sup>*jaewan@kriss.re.kr*

<sup>1</sup>*\*soohyun@kaist.ac.kr*

**Abstract:** An interferometer having resolution fourteen times higher than a conventional single-pass interferometer has been developed by creating multiple-pass optical path. To embody the multiple-pass optical configuration, a two-dimensional corner cube array block was designed, where its symmetric structure minimized the measurement error. The effect from the alignment error and the imperfection of corner cube is calculated and is in picometer level. An experiment proves that the proposed interferometer has optical resolution of approximate 45 nm and its nonlinearity is about 0.5 nm in peak-to-valley value.

©2009 Optical Society of America

**OCIS codes:** (120.0120) Instrumentation, measurement, and metrology; (120.3180) Interferometry

---

## References and links

1. T. Ito and S. Okazaki, "Pushing the limits of lithography," *Nature* **406**(6799), 1027-1031 (2000).
2. M. Totzeck, W. Ulrich, A. Göhnermeier and W. Kaiser, "Semiconductor fabrication - Pushing deep ultraviolet lithography to its limits," *Nat. Photonics* **1**, 629-631 (2007).
3. M. Pisani, "Multiple reflection Michelson interferometer with picometer resolution," *Opt. Express* **16**(26), 21558-21563, (2008).
4. H. Haitjema, P. H. J. Schellekens and S. F. C. L. Wetzels, "Calibration of displacement sensors up to 300  $\mu\text{m}$  with nanometer accuracy and direct traceability to a primary standard of length," *Metrologia*, **37**, 25-33 (2000).
5. M. J. Downs and W. R. C. Rowley, "A proposed design for a polarization-insensitive optical interferometer system with subnanometric capability," *Precis. Eng.* **15**(4), 281-286 (1993).
6. T. B. Eom, J. Y. Kim and K. Jeong, "The dynamic compensation of nonlinearity in a homodyne laser interferometer," *Meas. Sci. Technol.* **12**, 1734-1738 (2001).
7. P. L. M. Heydemann, "Determination and correction of quadrature fringe measurement errors in interferometers," *Appl. Opt.* **20**, 3382-3384 (1981).
8. EMRP T3.J1.4.NANOTRACE "New traceability routes for nanometrology," [www.emrpoline.eu](http://www.emrpoline.eu).
9. B. C. Park, T. B. Eom and M. S. Chung, "Polarization properties of cube-corner retroreflectors and their effects on signal strength and nonlinearity in heterodyne interferometers," *Appl. Opt.* **35**(22), 4372-4380 (1996).
10. G D'Agostino, A Germak, S Desogus, C Origlia and G Barboto, "A method to estimate the time-position coordinates of a free-falling test mass in absolute gravimetry," *Metrologia*, **42**, 233-238 (2005).

---

## 1. Introduction

Recently, as nano science and nano technology are advancing, demand for measuring the object of nanometer scale is increasing [1-2]. As standard equipment for nano scale measurement or semiconductor equipment, a laser interferometer has been widely used. The laser interferometer measures the displacement by referring to the wavelength so that it is traceable to the definition of meter, and it has nanometer resolution. However, more reliable and standard interferometer is needed when a picometer resolution is required. The reference wavelength of existing laser interferometers is about hundreds of nanometers. Dividing the interference signal electrically to increase the resolution until picometer level is difficult due

to the quantum noise limit, nonlinear error and electrical noise [3]. For this reason, many approaches, such as realignment of optical configuration [3-4], specially designed electronics and nonlinearity compensation algorithms [5-7] have been used to improve the performance of interferometers. The European community is also conducting a joint research project to realizing the sub-nanometer standard, and one of the main issues of the project is to increase the resolution of interferometers [8].

Theoretically, as the number of passes in the interferometer configuration increases, the optical resolution of the interferometer increases linearly. However, due to the complexity in setting up a multiple-pass optical configuration, the quadruple-pass has been considered as the reasonable limit when we increase the number of passes of the interferometer. Multiple reflection Michelson interferometer with picometer resolution has also been introduced [3]. It uses two plane mirrors, and one of them is inclined to the other for making multiple reflections. However, it can measure only short range for a finite size of mirrors, and it is very sensitive to the yaw motion of the stage because it is strongly dependent on the angular alignment.

This paper introduces a simple multiple-pass configuration using two-dimensional corner cube array, which is insensitive to the yaw and pitch motion of the stage. By changing the shape or size of the array, the optical resolution of interferometer can be adjusted. Using Zemax software, the measurement accuracy is estimated under the condition of expectable error sources.

## 2. Principle and optical configuration

Figure 1 shows a simple diagram of a multiple-pass interferometer. The incident beam is divided at the polarization beam splitter (PBS), so that some goes to reference arm and the other propagates to the target arm. Both of them first pass through a quarter wave plate (QWP), the axis of which is aligned at  $45^\circ$  to the polarization axes of the propagating beams.

In the target arm, there are two corner cube array (CCA) blocks, moving and fixed CCA blocks. The moving CCA block moves back and forth and behaves like a target mirror in the general interferometer, while the fixed CCA block just reflects the beam towards the moving CCA block again. At first, the laser beam exiting the PBS reaches the first corner cube,  $CC_1$ , in the moving CCA block, and is reflected toward to the second corner cube,  $CC_2$ , in the fixed CCA block. This completes a single-pass configuration.

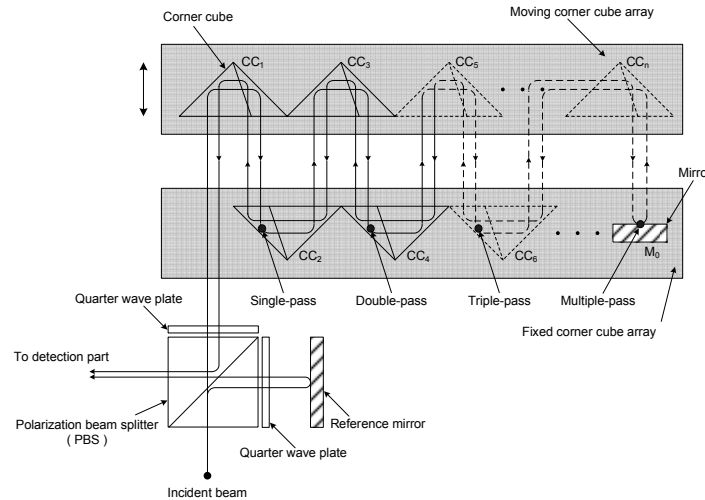


Fig. 1. Simple diagram of multiple pass interferometer

Consequently, the beam reflects at the  $CC_2$  again, and propagates to the third corner cube,  $CC_3$ . After passing the  $CC_3$  and arriving at the  $CC_4$ , the optical path becomes double-pass. In

the same manner, experiencing a pair of corner cubes makes a further number of passes, which means higher optical resolution of the interferometer. Figure 1 does not show the exact number of corner cubes, because additional corner cubes can be added or removed if it is necessary.

The mirror,  $M_0$  in the fixed CCA block is for making the exact reverse optical path to the PBS. Initially, the mirror,  $M_0$  is aligned perpendicular to the incident beam, so that the reflected beam is supposed to experience the same optical path toward the PBS but in opposite direction. On the other hand, the reference beam also reflects from the reference mirror and goes back to the PBS. Finally, the measurement beam and reference beam join at the PBS and move to the detection part.

As mentioned above, in this multiple-pass configuration the resolution of interferometer is determined by the number of corner cubes. The more corner cubes added, the higher resolution obtained. However, increasing the number of pass infinitely is impossible due to the intensity loss. A corner cube has about 95 % reflectivity when the incident beam reflects at the three surfaces of a corner cube by total internal reflection. However, that reflection induces the phase delay according to the angle between the polarization axis of the incident beam and the reference axis of the corner cube. Therefore, the exit beam experiences some changes in its polarization state. The uncoated corner cube can cause the elliptically polarized beam by relative phase retardation, about  $38^\circ$ , in the worst case. On the contrary, aluminum-coated corner cubes only have  $1.4^\circ$  of phase change [9].

To minimize the change of the polarization property, metal-coated corner cubes were suggested which have about 90 % reflectivity. In the configuration of Fig. 1, to get n-times higher resolution, the incident beam should experience  $2(n-1)$  corner cube reflections. For example, in the case of a 20-times higher resolution interferometer, 38 metal-coated corner cube reflections are expected. After those reflections, 2 % of light is detected at a photo diode. Assuming that the power of the stabilized He-Ne laser is more than 1 mW at least, 2 % of that, 20  $\mu$ W is enough to obtain the displacement information from it. Therefore, at least 20-times higher resolution interferometer is easily implemented by using a conventional metal-coated corner cube.

Arranging corner cubes just in a direction as shown in Fig. 1, however, makes the CCA block too long to be installed on the small-sized stage or narrow space. Considering such asymmetry, a new configuration is suggested in the next chapter.

### 3. Two-dimensional corner cube array

The change in configuration from Fig. 1 is that the moving and the fixed CCA block have two-dimensional arrangement of corner cubes. Figures 2(a) and 2(b) represent the configuration and optical path of the laser beam. In the moving CCA block, one corner cube locates on the center of the block, and the other six corner cubes are on the periphery of a circle so that seven corner cubes are aligned in symmetry. All beam positions are also placed on a circle line, and each of them has the uniform angular span,  $30^\circ$ . The fixed CCA block includes six corner cubes and one mirror, and their position is determined to make all beam positions locate symmetrically in a circumference. In Fig. 2(a), the  $CC_2$  induces the incident beam to go from 'b' in  $CC_1$  to position 'c' in  $CC_3$ . The order of beam propagation before the mirror,  $M_0$  is from 'a' to 'n' in alphabetical order, as shown in Fig. 2 (a). After the incident beam reflects at the mirror  $M_0$ , it takes the exact reverse path to arrive at position 'a' in the fixed CCA block. In passing by all the components, the beam completed a fourteen-pass. Therefore, the optical resolution becomes  $\lambda/28$ , which is fourteen times higher than that of a single-pass interferometer. More or less than 13 corner cubes can be used to make different number of passes, however, considering the size of a conventional corner cube and the symmetry, this new configuration has been suggested.

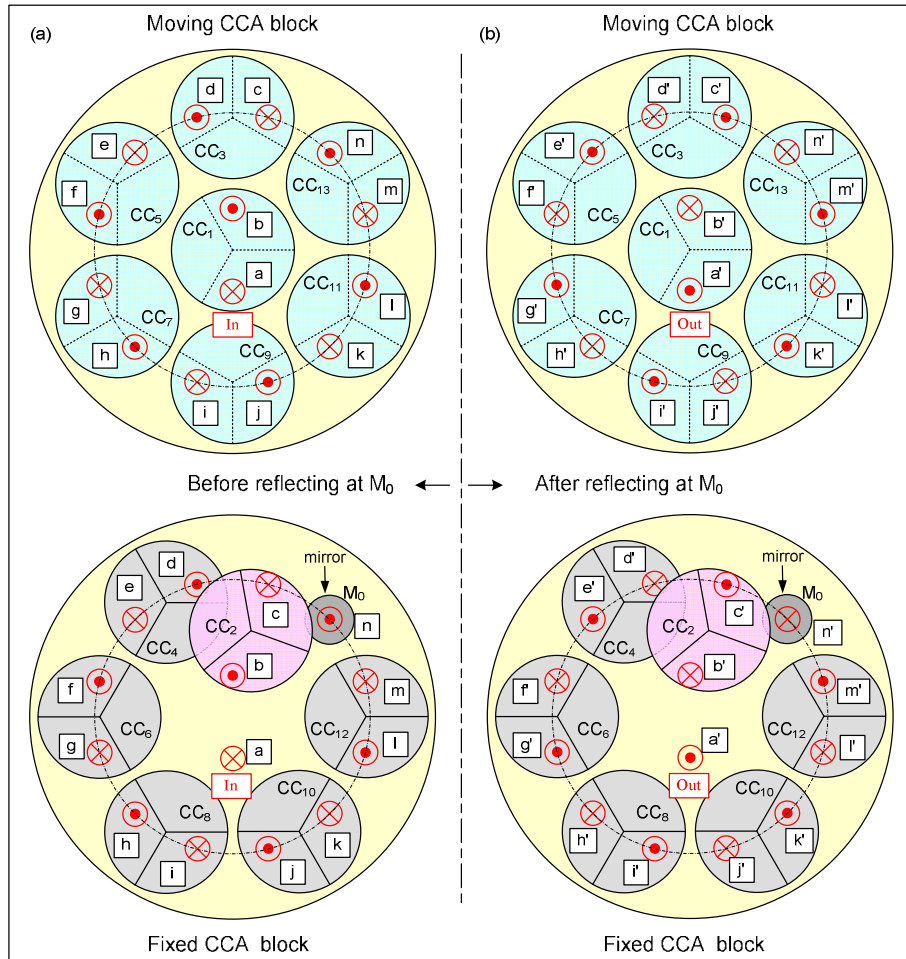


Fig. 2. Arrangement of corner cubes and beam path in the two-dimensional CCA configuration  
 (a) before the incident beam reflects at  $M_0$  [ path order :  
 $a \rightarrow b \rightarrow c \rightarrow d \rightarrow e \rightarrow f \rightarrow g \rightarrow h \rightarrow i \rightarrow j \rightarrow k \rightarrow l \rightarrow m \rightarrow n$  ]  
 (b) after the incident beam reflects at  $M_0$  [ path order :  
 $n' \rightarrow m' \rightarrow l' \rightarrow k' \rightarrow j' \rightarrow i' \rightarrow h' \rightarrow g' \rightarrow f' \rightarrow e' \rightarrow d' \rightarrow c' \rightarrow b' \rightarrow a'$  ]

The corner cube has an angular deviation as its imperfection in manufacturing, which means the exit light is not parallel to the incident beam. However, a corner cube of high quality only has  $2''$  of angular deviation so that the beam shifts only  $9 \mu\text{m}$  from the originally targeted position when it travels 10 m. Also, the angular deviation of a corner cube can be positive or negative, and this can be determined by interfering the two beams – one is reflecting from the front surface of a corner cube, and the other from total internal reflection. Therefore, if we combine them properly, we can reduce the total angular deviation of the CCA less than that of a single corner cube. Besides, the total path length of the suggested interferometer is much shorter than 10 m. Consequently, the angular deviation due to corner cubes is negligible when considering such a high-quality corner cube and adequate combination.

The symmetric configuration is robust to the measurement error from the yaw and pitch motion of the stage. Although the moving CCA block rotates  $\theta$  as in Fig. 3, the total path length does not change, because the increased path length on the left side corresponds to the decreased path length in the right side, the total path length is  $(2n+1)l$  regardless of rotation.  $n$  is the number of passes and  $l$  is the distance at the center position of the CCA block. Therefore,

the interferometer just measures the average distance,  $l$  due to the symmetric arrangement of corner cubes.

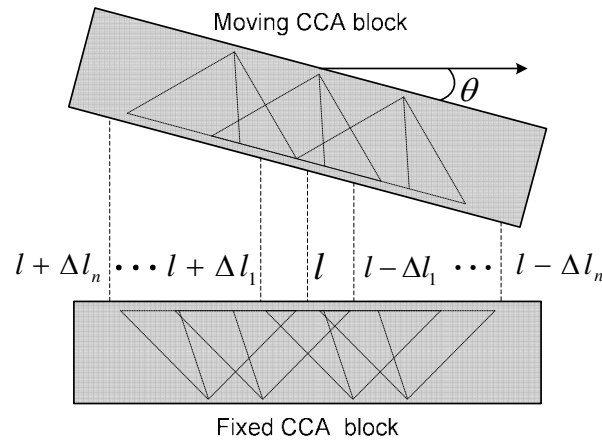


Fig. 3. Path length variation due to the rotation of moving CCA block

#### 4. Analysis

To determine the robustness of the measurement result to the yaw and pitch motion, a simulation was conducted using ZEMAX software. A 3D drawing of the multiple-pass interferometer was conducted and it was imported into ZEMAX for ray tracing at various conditions. Letting an incident beam with a 5 mm of diameter enter the CCA blocks at point 'a' in Fig. 2(a), the incident beam travels the planned path and comes out the CCA blocks at point 'b'. Figure 4 represents the path length variation due to the yaw and pitch motion of stage. Usually a fine motion stage has yaw and pitch motion of less than 10 arcsec, which can be improved according to the stage design and manufacture. When the yaw and pitch motion are less than 10 arcsec, the path length changes within sub nanometer as shown in Fig. 4. The curve for pitch motion has a bump covering the range from 0 to 15 arcsec. This is caused by the position of  $CC_2$  in the fixed CCA block. It is near the vertical axis, but it is far from the horizontal axis and placed asymmetrically compared with other CCs. Therefore, the curve for pitch motion is not symmetric as shown in that figure.

We also need to consider the beam position shift for the yaw and pitch motion. This can be determined using the same software. For 20 arcsec angular deviation, the beam position at  $M_0$  in the fixed CCA block only moves  $2.5 \mu\text{m}$ . This makes the overlap area – the reference beam and the measurement beam overlap at the entrance of detection part –  $1.8 \times 10^{-5} \%$  smaller than previously in the case of a 5 mm beam diameter, but it is not significant enough to affect the measurement result.

The dead path is almost 500 mm and brings a measurement error due to the refractive index variation of the air and the wavelength instability of the light source. The suggested multiple-pass interferometer, however, has distinction from the single-pass interferometer, which the same length of the dead path. Because the optical path is folded 14 times, the ray in the suggested interferometer only propagates in a specific and small region. Because of this, the dead path can be considered as shorter than 50 mm. Therefore, the effect of the refractive index variation does not increase as much as that of a single-pass interferometer. In addition, such a system, which requires sub-nanometer or higher resolution, should be isolated from the environment error sources not to deteriorate its original measuring capability. For example, the vacuum chamber with temperature control equipment and a stabilized He-Ne laser source is helpful to overcome the dead path error.

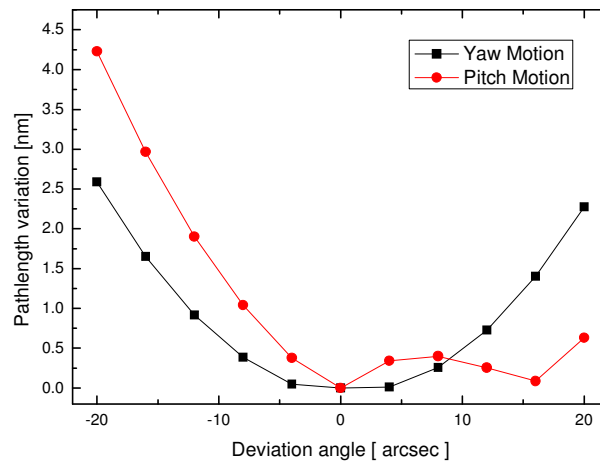


Fig. 4. Path length variation due to the yaw and pitch motion of stage

## 5. Experiments & Result

To verify the enhanced resolution of the multiple-pass interferometer, a simple experimental setup is established (see Fig. 5). A stabilized He-Ne laser is adopted as a light source, and to compensate its beam divergence, a beam expander is placed after the isolator. To minimize the change of polarization at corner cube reflection, aluminum-coated corner cubes are used. However, its reflectivity was known to about 90 %, which is 5 % lower than that of an uncoated corner cube. In this configuration, through the target arm, the incident beam experiences 26 reflections and one mirror reflection, this results in a 5 % intensity transmission to the detection part. Therefore, considering the intensity loss, we need to distribute the light intensity differently to the reference arm and the target arm. The half wave plate (HWP) just before the PBS rotates the linear polarization axis so that about 95 % of intensity can transmit to the target arm.

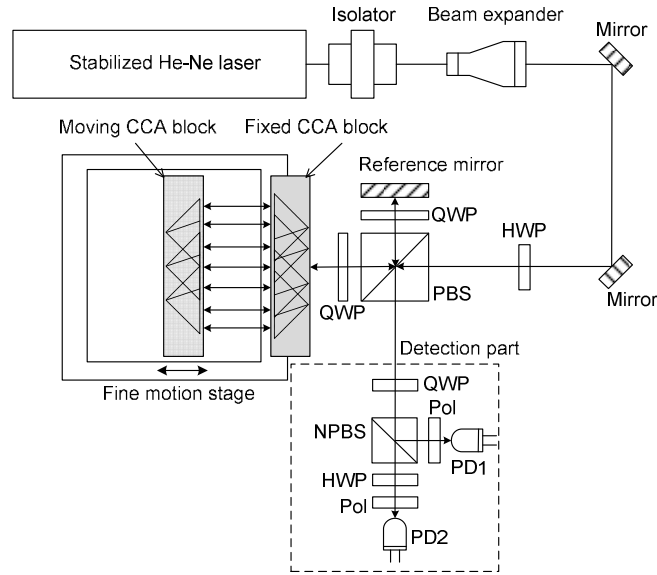


Fig. 5. Simple diagram of experiment setup (HWP: Half Wave Plate, PBS: Polarization Beam Splitter, QWP: Quarter Wave Plate, NPBS: Non-Polarization Beam Splitter, Pol: Polarizer, PD: Photo Diode).

Finally, the two beams from the reference and target arm have the same intensity at the entrance to the detection part. The axes of QWPs are aligned at  $45^\circ$  to the polarization axis of the beam to make  $90^\circ$  of polarization change by passing it twice. To demonstrate the basic principle and the performance of a multiple pass interferometer, a fine motion stage having hundreds of  $\mu\text{m}$  stroke range is used, and 0.1 Hz triangle wave is applied to operate it. The detection part includes optical elements for the quadrature detection method, which uses two sinusoidal signals having  $90^\circ$  of phase difference.

The fine motion stage moves about 160 nm, which results in a half cycle of the interferogram in the case of a single-pass interferometer. However, this fourteen-pass interferometer has seven cycles during that displacement as shown in Fig. 6. The mean value is abstracted from the raw data to make the offset zero, after that the intensity is normalized by making the amplitude a unit.

Nonlinearity is the practical limitation in the measuring capability of the interferometer when other environmental error sources are under control. In principle, multiple-pass interferometer has smaller nonlinear error than that of single-pass interferometer, because when calculating the displacement from the phase signal, the number of passes divides the phase error, too.

For the suggested multiple-pass interferometer, there will be polarization mixing due to the corner cube reflections. This induces the phase error in the final interferometer signals. Considering that  $1.4^\circ$  of phase change during the reflection at the aluminum-coated corner cube, the multiple-pass interferometer can have a nonlinearity of about 1.23 nm, excepting other nonlinearity sources only due to the imperfection of corner cubes. However, careful alignment of the corner cubes can avoid such worst case and will give the same magnitude of nonlinearity as that of a single-pass interferometer. Therefore, when we consider that the nonlinearity of a single-pass interferometer is about 3 ~ 4 nm, the fourteen-pass interferometer will have sub-nanometer nonlinearity. To determine the nonlinearity from the data in Fig. 6, one period of interference signal is chosen for calculation. The displacement of a CCA block can be acquired by using the selected data. The movement of a PZT stage is not linear to the applied voltage for the nonlinear characteristic of a piezo actuator. Therefore, fitting the displacement curve to the third polynomial for the applied voltage gives a characteristic curve of piezo actuator. The nonlinearity of the interferometer can be obtained by subtracting the

characteristic curve from the calculated displacement curve. Through this procedure, the nonlinearity was acquired for one period of interference signal, and it was about 0.5 nm in peak-to-valley. As expected this, the multiple-pass interferometer shows out the reduced nonlinearity when we consider the nonlinearity of single-pass interferometer

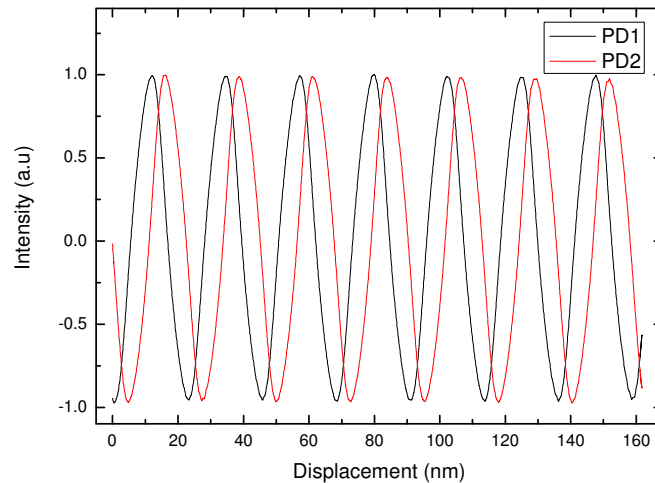


Fig. 6. Periodic signal according to the displacement of fine motion stage

## 6. Summary

A new multiple-pass interferometer has been suggested by using a two-dimensional corner cube array. Its optical resolution is 14 times higher than that of a conventional single pass interferometer. Through an experiment the resolution of the suggested multiple-pass interferometer has been proved to be 45 nm, and its nonlinearity about 0.5 nm. The CCA block has a symmetric structure so that the interferometer is robust to the yaw and pitch motion of the stage and other environmental error sources. The error by the long dead path can be minimized in the vacuum chamber. Measuring the acceleration of gravity in the vacuum chamber can be one of those applications, which require high resolution and rapid measuring [10].

## Acknowledgements

This work was supported by Korea Science & Engineering Foundation through the Nano R&D Program (Grant 2009-0082848).